

Rotation of the pre-stellar core L1689B

M.P. Redman^{1,2}, E. Keto³, J.M.C. Rawlings¹, D.A. Williams¹

¹*Department of Physics and Astronomy, University College London, Gower Street, London WC1E 6BT, UK*

²*School of Cosmic Physics, Dublin Institute for Advanced Studies, 5 Merrion Square, Dublin 2, Republic of Ireland*

³*Harvard-Smithsonian Center for Astrophysics, 60 Garden Street, Cambridge MA 02138, USA*

27 October 2018

ABSTRACT

The search for the onset of star formation in pre-stellar cores has focussed on the identification of an infall signature in the molecular line profiles of tracer species. The classic infall signature is a double peaked line profile with an asymmetry in the strength of the peaks such that the blue peak is stronger. L1689B is a pre-stellar core and infall candidate but new JCMT HCO⁺ line profile data, presented here, confirms that both blue and red asymmetric line profiles are present in this source. Moreover, a dividing line can be drawn between the locations where each type of profile is found. It is argued that it is unlikely that the line profiles can be interpreted with simple models of infall or outflow and that rotation of the inner regions is the most likely explanation. A rotational model is developed in detail with a new 3D molecular line transport code and it is found that the best type of model is one in which the rotational velocity profile is in between solid body and Keplerian. It is firstly shown that red and blue asymmetric line profiles can be generated with a rotation model entirely in the absence of any infall motion. The model is then quantitatively compared with the JCMT data and an iteration over a range of parameters is performed to minimize the difference between the data and model. The results indicate that rotation can dominate the line profile shape even before the onset of infall.

Key words: radiative transfer - submillimetre - stars: formation - ISM: clouds - ISM: molecules - ISM: individual: L1689B

1 INTRODUCTION

The physics of the collapse process that leads to the formation of a star is still not understood. Although many models of star formation have been proposed, observational difficulties have limited the degree to which they can be tested. Molecular line profiles, emitted in the mm and sub-mm regimes, potentially offer the best opportunity to extract dynamical information about the collapse process that leads to the formation of stars. For some species the abundances are great enough that self-absorption of the line takes place and if the gas is undergoing infall then the line can assume a characteristic double-peaked profile with a stronger blue wing. Evans (1999) has reviewed how such line profiles are generated and this is discussed further below. Much observational effort has been concentrated on detecting and characterising blue asymmetric line profiles in the hope of using them to extract dynamical information. For example, Choi et al. (1995) and Zhou et al. (1993) modelled the pre-stellar core B335 as undergoing a Shu (1977) ‘inside-out’ collapse. However, the observational data in these cases consisted of one or a few molecular lines at a single position in the cloud. Though a consistent fit to the data could be made using a Shu collapse model there was no

guarantee that the fit was unique and Wilner et al. (2000) showed that such a model was not able to explain their CS (5 – 4) data of B335. While the search for infall in pre-stellar cores has become focussed on identifying blue asymmetric line profiles, it is becoming clear that the interpretation of the molecular line profiles from collapse candidates is much more complex than previously thought with the shape of the line profile being highly sensitive to the chemical and physical properties of the gas (e.g. Rawlings & Yates 2001; Ward-Thompson & Buckley 2001).

In this paper, an additional possible cause of asymmetric line profiles is considered: rotation, which is suggested by the observed spatial separation of red and blue asymmetric profiles in JCMT line profiles obtained from the pre-stellar core L1689B, reported below. L1689B is modelled as a system in which the central regions are dynamically active and undergoing rotation while the outer regions are quiescent. A 3D molecular line transport code is employed to model the core and to directly compare the results with recently obtained JCMT data. In Section 2 observations of L1689B are reviewed and the JCMT data that is to be modelled is presented. The model and code are described in Section 3. The results are presented and discussed in Section 4

and compared with other recent studies, particularly that of Belloche et al. (2003) who have recently demonstrated the presence of rotation in the more evolved Class 0 source, IRAM 04191+1522. It is concluded in Section 5 that the asymmetric line profiles can be very well modelled if L1689B is undergoing rotation and that therefore rotation dominates any infall motions in this source.

2 THE PRE-STELLAR CORE L1689B

L1689B is a pre-stellar core located in Ophiuchus. Shirley et al. (2000) present SCUBA maps of L1689B that confirm that there is no protostellar object in the centre of the core. Evans et al. (2001) use a self-consistent dust emission model to constrain the properties of L1689B and conclude that the dust temperature decreases from the edge to the centre, a conclusion also reached by André et al. (1996) and Jessop & Ward-Thompson (2001). The density structure of the core is mildly flattened in the centre and decreases for larger radii. The density was well modelled by Evans et al. (2001) using a Bonner-Ebert sphere density distribution (see e.g. McLaughlin & Pudritz 1996; Alves et al. 2001; Evans et al. 2001; Whitworth & Ward-Thompson 2001; Wuchterl & Tscharnuter 2003 for recent work involving Bonner-Ebert spheres).

Redman et al. (2002) carried out $C^{17}O$ $J = 2 \rightarrow 1$ observations towards the pre-stellar core L1689B. By examining the relative strengths of the hyperfine components of this line the optical depth was calculated. This allowed accurate CO column densities to be determined. The hydrogen column densities that these measurements imply are substantially smaller than those calculated from SCUBA dust emission data of Shirley et al. (2000) and Evans et al. (2001). Furthermore, the $C^{17}O$ $J = 2 \rightarrow 1$ column densities are approximately constant across L1689B whereas the SCUBA column densities are peaked towards the centre. The most likely explanation is that CO is depleted from the central regions of L1689B, as also suggested by Jessop & Ward-Thompson (2001). Evidence of CO depletion has also been found in several other prestellar cores (Caselli et al. 1999; Bacmann et al. 2002; Jørgensen et al. 2002; Tafalla et al. 2002). It was estimated by Redman et al. (2002) that within about 5000 AU of the centre of L1689B, over 90% of the CO has frozen onto grains. This level of depletion can only be achieved after a duration of time that is at least comparable to the free-fall timescale. While the CO emitting gas appears to be quiescent, line profiles obtained by Gregersen & Evans (2000) show the presence of both blue *and* red asymmetric line profiles in this source. New JCMT observations, described below, confirm the observational results of Gregersen & Evans (2000) and reveal an underlying order to the locations of the blue and red asymmetric profiles.

3 JCMT OBSERVATIONS OF L1689B

The bulk of the observations were carried out using the heterodyne receiver RxA3 at the James Clark Maxwell Telescope (JCMT), Mauna Kea, Hawaii on the nights of 2001 February 24-26, 2001 August 19-21, 2003 May 3-5.

Additional data were collected on various dates in 2001. HCO^+ $J = 3 \rightarrow 2$ (267.5665 GHz) line profiles were obtained for seventeen positions across the centre of L1689B. Some of the data points were collected as part of a larger survey of infall candidate objects, the results of which will be reported in Redman et al. (2004). The data were reduced in the standard manner using the SPECX software package and were converted to the T_{mb} scale using a main beam efficiency of 0.7.

The seventeen positions are at different offsets and at shorter spacings than those of Gregersen & Evans (2000). The line profiles are displayed in Fig 1. Again, the presence of both blue and red asymmetric line profiles is apparent. The two datasets cover different, though overlapping, parts of the cloud (note that, as is often the case for prestellar cores, the position of the centre of the cloud is somewhat uncertain - see, e.g., the SCUBA dust emission map of Shirley et al 2000). While in our map the majority of the profiles are red asymmetric line profiles, the opposite is the case for the Gregersen & Evans (2000) dataset. Where the pointing positions between the Gregersen & Evans (2000) dataset and the present study overlap (in the north-east [top right] corner) it was verified that the datasets match each other.

Inspection of the data of Gregersen & Evans (2000) and Fig 1 reveals that the blue and red asymmetric line profiles are found on either side of an axis that runs from SW to NE. This axis is displaced to the NW of the zero offset position of our dataset but would run through the centre of the combined datasets. The change in asymmetry is in broad accord with the lower spatial resolution CS $2 \rightarrow 1$ data of Lee et al. (1999) (obtained with FCRAO) in which the sense of asymmetry of the line profiles switches from blue in the north of L1689B to red in the south. This indicates that there is dynamical activity in the HCO^+ emitting gas. Since the outer layers of the cloud, as traced by $C^{17}O$, are quiescent (the hyperfine structure is well resolved - Redman et al. 2002) the dynamically active gas must lie within the CO depleted region.

4 MODELLING

A blue asymmetric line profile in an infalling core will be formed if (i) the infall velocity increases less slowly than $1/r$ and (ii) the excitation temperature increases towards the centre (e.g. Evans 1999). The dust radiative transfer modelling carried out by Evans et al. (2001) demonstrates that the second of these conditions may not be met in an object like L1689B since the dust temperature (and, if they are well coupled, the gas temperature) decreases towards the centre of the cloud. Furthermore, of course, the presence of red asymmetric line profiles as well as blue asymmetric profiles toward the centre of the cloud means that simple infall cannot explain the observational data.

Since star formation is usually accompanied by outflows, one possible explanation is that an outflow is the cause of the changes in the sense of the asymmetry. However, this can be discounted here since the CO would be kinematically disturbed and the sharply resolved hyperfine structure would be blended away. Furthermore, in a starless core with an interior depleted in heavy molecules, such as L1689B, an outflow is not yet expected to have been initiated. Instead,

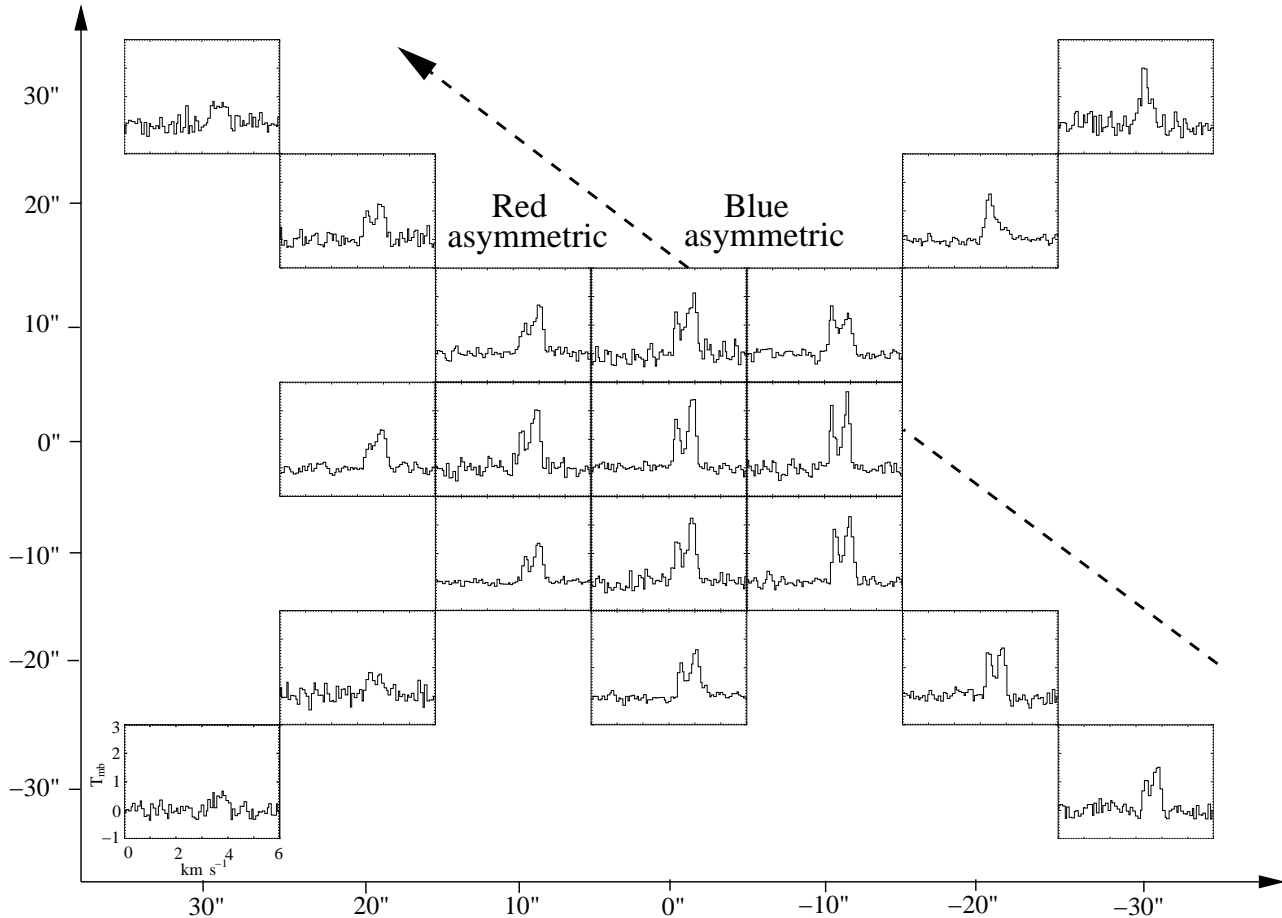


Figure 1. HCO^+ $J = 3 \rightarrow 2$ line profiles from positions across the centre of L1689B. The coordinates of the pointing centre are RA 16 31 47.0, DEC -24 31 45.0 (B1950). The axis dividing blue and red asymmetric profiles is displaced to the NW of the zero offset position of our dataset

we model the system as consisting of a quiescent outer halo where the CO is emitted, with a rotating inner HCO^+ emitting region. Figure 2 is a sketch of the model.

4.1 General description of the code

In dark molecular clouds, the density is usually too low for local thermodynamic equilibrium (LTE) to apply, the opacity is usually too high for an optically thin approximation and the systemic velocities are too low for the large velocity gradient (LVG) or Sobolev approximations to be valid. We therefore generate model spectra and intensity maps using a non-LTE numerical radiative transfer code (described in Keto et al. 2003 and also used by Rawlings et al. 2004). The code is fully 3 dimensional and employs the accelerated lambda iteration (ALI) algorithm of Rybicki & Hummer (1991) to solve the molecular line transport problem within an object of arbitrary (three-dimensional) geometry. This represents a considerable improvement over the early models of Keto (1990).

The local line profile is specified by systemic line-of-sight motions together with thermal and turbulent broadening. In addition to essential molecular data (such as collisional excitation rates) the physical input to the model consists of the three-dimensional velocity, density and temper-

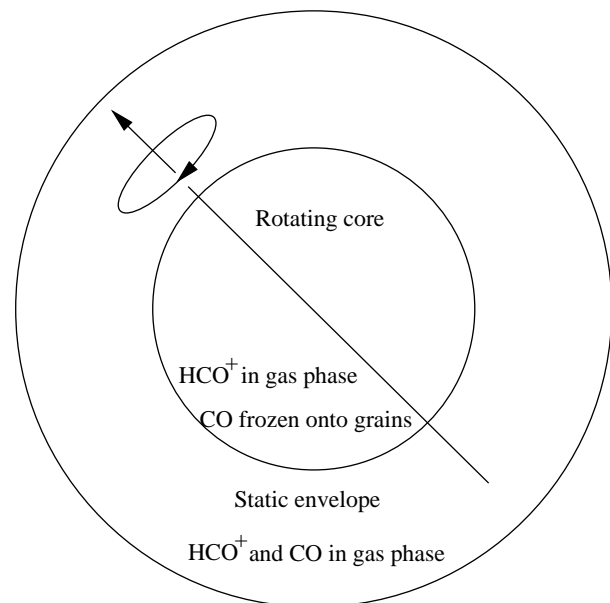


Figure 2. Sketch of the model of L1689B. The radius of the rotating centre is 3000 AU. Redman et al. (2002) estimated that most of the CO is frozen onto grains within the central 5000 AU

ature structures. The radiative transfer equations are then numerically integrated over a grid of points representing sky positions. The main source of uncertainty in the radiative transfer calculations are the collisional rate coefficients, but this should only be manifest in the uncertainties in the line strengths (which may be inaccurate by as much as 25%); the line profile shapes and relative strengths should be less affected.

For our purposes we define a spherical cloud within a regularly spaced cartesian grid of $30 \times 30 \times 30$ cells. Within each cell, the temperature, H_2 density, molecular species abundance, turbulent velocity width, and bulk velocity are specified. Externally, the ambient radiation field is taken to be the cosmic microwave background. At a given viewing angle to the grid, the line profile is calculated at specified offsets from the centre by integrating the emission along the lines of sight. It is then possible to regrid the data in the map plane and convolve with the (typically Gaussian) beam pattern of the telescope, which for the JCMT is $15''$. The spectra are computed with a frequency resolution of 0.01 km s^{-1} .

4.2 Comparison with observational data

Once a plausible general model has been set up, observational data can be read directly into the code and multiple models with varying parameters can be calculated and the difference between the model and the data minimized. The dimension of the model cube is selected so that the data points are positioned at integer values of the cube spacing. The data is regridded so that the data channels match those of the model output. After generating a model cube, the code compares the model with the data and calculates χ^2 for that fit. The numerical techniques of simplex and simulated annealing are used to drive the refining process where the code adopts new parameters and calculates a new cube; full details are given in Keto et al. (2003). A typical fitting run may require the calculation of several hundred model cubes.

4.3 L1689B model

The model parameters are listed in Table 4.3 along with either the fixed adopted values used in the code or the range over which a parameter was allowed to vary. The number of model runs required to explore the parameter space increases rapidly with the number of free parameters so those parameters which have the best empirical constraints were given fixed values.

The density profile used is that of a Plummer sphere which is defined as

$$\rho(r) = \frac{\rho_0 r_0^2}{r^2 + r_0^2} \quad (1)$$

where ρ_0 is the central density and r_0 is the Plummer radius. This simple density law has the property that as $r \rightarrow 0$, $\rho(r) \rightarrow \rho_0$ while for large r , $\rho(r) \rightarrow \rho_0/r^2$. The outer radius of the cloud is defined as 6000 AU. The Plummer profile is also a reasonable approximation to (and easier to deal with than) the Bonner-Ebert sphere density distribution. This latter distribution appears to describe the density profile of

Parameter	Adopted value or range (best fit value)
Outer radius	6000 AU
Plummer radius r_0	1000 AU
Plummer density ρ_0	10^6 cm^{-3}
Temperature	10 K (edge) - 7 K (centre)
HCO^+ abundance	$5.0 \times 10^{-10} - 1.0 \times 10^{-8}$ (7.84×10^{-9})
Projected velocity	$0.1 - 0.4 \text{ km s}^{-1}$ (0.121)
Rotation radius	3000 AU
Turbulent velocity	$0.12 - 0.18 \text{ km s}^{-1}$ (0.157)

Table 1. Model parameters used. For the parameters that were allowed to vary, the best fit value is given in brackets

pre-stellar cores and is beginning to be used routinely in modelling work. The adopted values of r_0 and ρ_0 were 1000 AU and 10^6 cm^{-3} respectively. These values were chosen to approximate the Bonner-Ebert sphere fit to the density distribution of L1689B carried out by Evans et al. (2001). Similarly, an empirical approximation to the dust temperature profile fit of Evans et al. (2001) was employed to trace the gas temperature (the gas density is sufficiently high that the two temperatures can be considered well coupled). The temperature is 10 K in most of the cloud and then drops, over a short distance, to 7 K in the centre. In fact, trial runs with a constant temperature of 10 K throughout the cloud yield very similar results to this temperature profile.

The fractional abundance of HCO^+ was taken to have a constant value from the range $5.0 \times 10^{-10} - 1.0 \times 10^{-8}$. The assumption of a constant abundance is of course a crude approximation and a self-consistent chemistry should be included in the cloud. However, the chemistry of HCO^+ is complicated and Rawlings et al. (1992) show that its abundance initially rises as depletion ensues. The sticking coefficient of HCO^+ on to charged and neutral dust grains is also not well known. Therefore an attempt to include the chemistry does not yet seem worthwhile.

A simple solid body rotation law was adopted for the inner regions of the model cloud. A rotation axis that matches the dividing line between the red and blue asymmetric profiles was imposed. The range of projected velocities investigated is $0.1 - 0.4 \text{ km s}^{-1}$. The rotation radius is an estimate of where the inner regions stop rotating and is estimated as being at 3000 AU (cf. 5000 AU for the CO depleted 'hole' Redman et al. 2002). Finally, the uncertain turbulent velocity width was allowed to vary over the range $0.12 - 0.18 \text{ km s}^{-1}$.

5 RESULTS AND DISCUSSION

The full set of synthesised $\text{HCO}^+ J = 3 \rightarrow 2$ line profiles for the best fit model is displayed in Figure 3. For clarity, the rotation axis points vertically. The line profiles show clear asymmetries with the sense of the asymmetry switching between red and blue on either side of the rotation axis. The self-absorption is strongest towards the centre of the model cloud and the asymmetry is strongest there. Away from the centre of the cloud, the drop in column density and self-absorption results in a reduced line strength and less pronounced asymmetry (the difference in strength between red and blue peak; the relative magnitude of the absorption trough). These results confirm that it is possible to

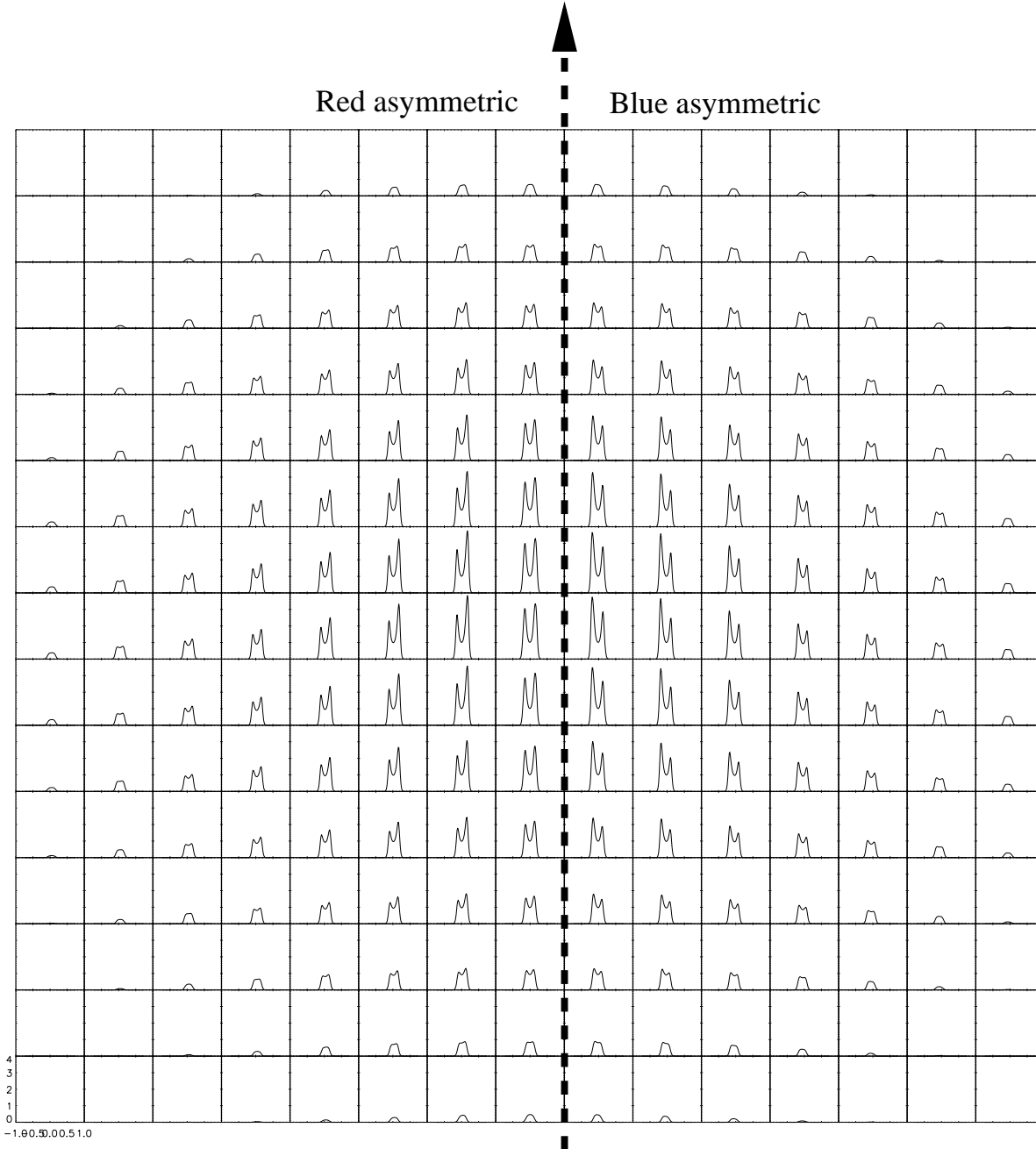


Figure 3. $\text{HCO}^+ J = 3 \rightarrow 2$ line profiles from the rotation model. For clarity the array of profiles is displayed with the rotation axis as shown. The line profiles switch between red asymmetric and blue asymmetric on either side of the rotation axis.

generate both red and blue asymmetric line profiles entirely in the absence of any infall or outflow motions.

Figure 4 is an overlay of the best fit model described above with the JCMT data of Redman et al (2004). The rotation axis is marked on the figure. Given the simplicity of the model, the fit is excellent with the sense of the asymmetry in the line profiles, their shape and the fall-off in line strength away from the centre being reproduced well. The most obvious of the discrepancies is that the line strengths are overestimated for the brightest lines near the centre of the cloud. One explanation for this may be due to the freez-

ing out of HCO^+ onto grains. Any freeze-out of the HCO^+ is likely to occur first in the centre of the cloud, where the density is highest, and progress outwards. If there is significant freeze-out in the very centre of the cloud, this would reduce the strength of the line profiles for small impact parameters. As noted above, the chemical behaviour of HCO^+ in a core undergoing depletion is complicated.

Belloche et al. (2003) have carried out a detailed study of the Class 0 protostar IRAM 04191+1522 and conclude that the inner region of IRAM 04191+1522 is undergoing fast differential rotation while the outer regions are only

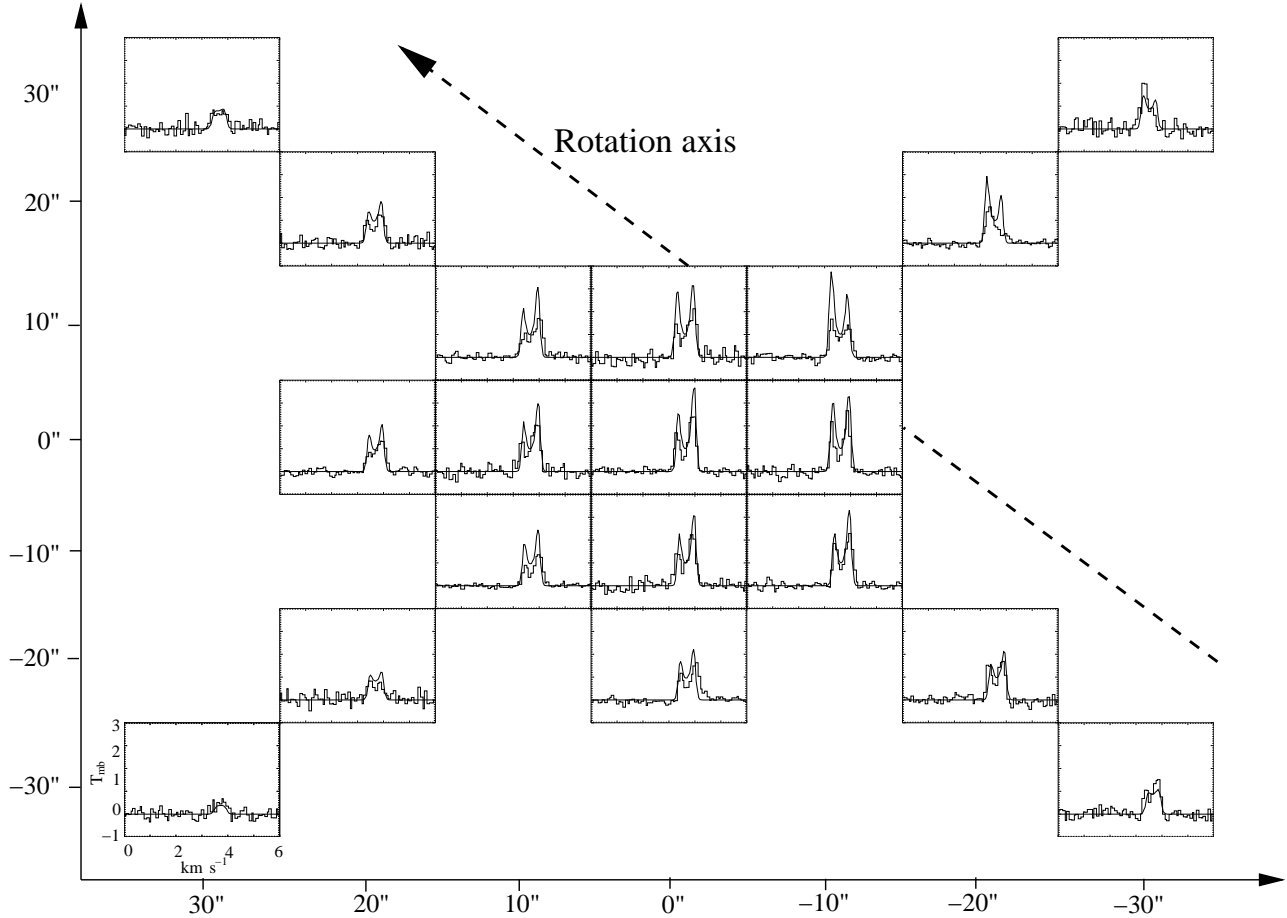


Figure 4. $\text{HCO}^+ J = 3 \rightarrow 2$ line profiles from L1689B. The spacing between the cells is $10''$. North is up and east is to the right. Overlaid are synthesised line profiles generated by the rotation model for the source.

slowly rotating. Since they also argue that this source has only recently become a protostar it is constructive to compare it with L1689B which may be on the verge of collapse. Firstly, under the assumption that both objects have been adequately modelled, the angular velocity is comparable: $\omega r = 9.4 \text{ km s}^{-1}$ at 3000 AU in the best fit model for L1689B while for IRAM 04191+1522, $\omega r = 9 \pm 3 \text{ km s}^{-1}$ at 2800 AU. IRAM 04191+1522 may be decoupling from the outer envelope at a radius of 2000-4000 AU (Belloche et al. 2003) which compares with the rotation radius of 3000 AU estimated here for L1689B. Solid body rotation is firmly ruled out for the inner region of IRAM 04191+1522 with differential rotation providing a much better fit to the observations (specifically, the angular velocity gradient is found to change from approximately $\omega \propto r^{-2.5}$ to $\omega \propto r^{-1}$ in the inner regions with very slow rotation in the outer regions). The model results presented here for L1689B also supports an $\omega \propto r^{-1}$ angular velocity profile. Such a velocity gradient indicates that angular momentum is conserved and that magnetic braking does not dominate the dynamics; Belloche et al. (2003) provide an extensive discussion of their results in terms of various collapse models. Thus, L1689B exhibits strong similarities with IRAM 04191+1522 in terms of the rotational behaviour. The principal kinematic difference is that IRAM 04191+1522 shows clear evidence of infall (and outflow) in addition to rotation yet the signature

of any such motion in L1689B is completely dominated by the rotation. It seems reasonable to suggest that L1689B and IRAM 04191+1522 are similar objects that are at slightly different evolutionary stages, either side of the onset of infall.

6 CONCLUSIONS

A model of the pre-stellar collapse candidate L1689B has been presented where the inner regions of the cloud are undergoing rotation while the outer part of the cloud is static and quiescent. The model calculations demonstrate that blue and red asymmetric line profiles arise naturally from such a system even in the absence of infall or outflowing gas motions. The possibility that rotation is present in a pre-stellar object must therefore be addressed if asymmetric line profiles are to be used to argue that a core is undergoing infall.

A best fit model was generated by varying several of the free parameters within reasonable ranges. An excellent fit to the data was obtained and we would therefore argue that our model is a plausible one for L1689B.

This study along with other recent work demonstrates that great care needs to be taken in interpreting asymmetric line profiles as evidence for infall. While this means that earlier claims for detection of infall (e.g. Zhou et al. 1990)

ought now be re-evaluated it does not mean the search will be fruitless. A combination of chemical models, radiative transfer codes and high quality observations should soon lead to the first firm identification of infall and the long awaited detailed examination of the competing star formation models.

ACKNOWLEDGEMENTS

MJR was funded by PPARC while this work was carried out. DAW acknowledges the support of the Leverhulme Trust. This work was partially supported by the National Science Foundation through a grant for the Institute for Theoretical Atomic, Molecular and Optical Physics at Harvard University and Smithsonian Astrophysical Observatory. We thank the staff of the JCMT for their excellent assistance during the observations. The JCMT is operated by the JAC, Hawaii, on behalf of the UK PPARC, the Netherlands NWO, and the Canadian NRC.

REFERENCES

- Alves J. F., Lada C. J., Lada E. A., 2001, *Nature*, 409, 159
 André P., Ward-Thompson D., Motte F., 1996, *A&A*, 314, 625
 Bacmann A., Lefloch B., Cecarelli C., et al 2002, *A&A*, 389, L6
 Belloche A., André P., Despois D., Blinder S., 2003, *A&A*, 393, 927
 Caselli P., Walmsley C. M., Tafalla M., Dore L., Myers P. C., 1999, *ApJ*, 523, L165
 Choi M., Evans II N. J., Gregersen E. M., Wang Y., 1995, *ApJ*, 448, 742
 Evans N. J., 1999, *ARA&A*, 37, 311
 Evans N. J., Rawlings J. M. C., Shirley Y. L., Mundy L. G., 2001, *ApJ*, 557, 193
 Gregersen E. M., Evans N. J., 2000, *ApJ*, 538, 260
 Jessop N. E., Ward-Thompson D., 2001, *MNRAS*, 323, 1025
 Jørgensen J. K., Schöier F. L., van Dishoeck E. F., 2002, *A&A*, in press
 Keto E., 1990, *ApJ*, 355, 190
 Keto E., Rybicki G., Plume R., 2003, *ApJ*, Submitted
 Lee C. W., Myers P. C., Tafalla M., 1999, *ApJ*, 526, 788
 Marti F., Noerdlinger P. D., 1977, *ApJ*, 215, 247
 McLaughlin D. E., Pudritz R. E., 1996, *ApJ*, 469, 194
 Rawlings J. M. C., Hartquist T. W., Menten K. M., Williams D. A., 1992, *MNRAS*, 255, 471
 Rawlings J. M. C., Redman M. P., Keto E., Williams D. A., 2004, *MNRAS*, Accepted
 Rawlings J. M. C., Yates J. A., 2001, *MNRAS*, 326, 1423
 Redman M. P., Rawlings J. M. C., Nutter D. J., Ward-Thompson D., Williams D. A., 2002, *MNRAS*, 337, L17
 Rybicki G. B., Hummer D. G., 1978, *ApJ*, 219, 654
 Rybicki G. B., Hummer D. G., 1991, *A&A*, 245, 171
 Shirley Y. L., Evans N. J., Rawlings J. M. C., Gregersen E., 2000, *ApJS*, 131, 249
 Shu F. H., 1977, *ApJ*, 214, 488
 Tafalla M., Myers P. C., Caselli P., Walmsley C. M., Comito C., 2002, *ApJ*, 569, 815
 Ward-Thompson D., Buckley H. D., 2001, *MNRAS*, 327, 955
 Whitworth A. P., Ward-Thompson D., 2001, *ApJ*, 547, 317
 Wilner D. J., Myers P. C., Mardones D., Tafalla M., 2000, *ApJ*, 544, L69
 Wuchterl G., Tscharnuter W. M., 2003, *A&A*, 398, 1081
 Young L. M., Keto E., Ho P. T. P., 1998, *ApJ*, 507, 270
 Zhou S., Evans N. J., Butner H. M., Kutner M. L., Leung C. M., Mundy L. G., 1990, *ApJ*, 363, 168
 Zhou S., Evans II N. J., Kömpe C., Walmsley C. M., 1993, *ApJ*, 404, 232